

# Ghost poles in the nucleon propagator in the linear $\sigma$ model approach and its role in $NN$ low-energy theorems

C. A. da Rocha<sup>(1)</sup>, G. Krein<sup>(2)y</sup>, and L. Wilets<sup>(1)z</sup>

(1) Department of Physics, Box 351560, University of Washington, Seattle, Washington 98195-1560

(2) Instituto de Física Teórica - Universidade Estadual Paulista - Rua Pamplona 145, 01405-900 São Paulo-SP, Brazil  
(January 1997)

Complex mass poles, or ghost poles, are present in the Hartree-Fock solution of the Schwinger-Dyson equation for the nucleon propagator in renormalizable models with Yukawa-type meson-nucleon couplings, as shown many years ago by Brown, Puff, and Wilets (BPW). These ghosts violate basic theorems of quantum field theory and their origin is related to the ultraviolet behavior of the model interactions. Recently, Krein et al, proved that the ghosts disappear when vertex corrections are included in a self-consistent way, softening the interaction sufficiently in the ultraviolet region. In previous studies of  $NN$  scattering using "dressed" nucleon propagator and bare vertices, did by Nutt and Wilets in the 70's (NW), it was found that if these poles are explicitly included, the value of the isospin-even amplitude  $A^{(+)}$  is satisfied within 20% at threshold. The absence of a theoretical explanation for the ghosts and the lack of chiral symmetry in these previous studies led us to re-investigate the subject using the approach of the linear  $\sigma$  model and study the interplay of low-energy theorems for  $NN$  scattering and ghost poles. For bare interaction vertices we find that ghosts are present in this model as well and that the  $A^{(+)}$  value is badly described. As a first approach to remove these complex poles, we dress the vertices with phenomenological form factors and a reasonable agreement with experiment is achieved. In order to fix the two cutoff parameters, we use the  $A^{(+)}$  value for the chiral limit ( $m \rightarrow 0$ ) and the experimental value of the isoscalar scattering length. Finally, we test our model by calculating the phase shifts for the S waves and we find a good agreement at threshold.

PACS number(s): 21.30.+y, 13.75.Gx, 11.30.Rd, 21.60.Jz

## I. INTRODUCTION

Elastic pion-nucleon ( $NN$ ) scattering has been studied for more than 40 years. The body of work until the early 80's was reviewed by Hohler [1]. In recent years a renewed interest in  $NN$  scattering is being witnessed [2,3,4] in the literature. This interest is driven mainly by the necessity of having a relativistic description of the available high energy data, as well as of the data to be generated at CEBAF. Also, the recognition of chiral symmetry as a fundamental symmetry of the strong interactions has motivated a great deal of attention to the role of this symmetry in the  $NN$  process. This last point is particularly interesting in view of the possibility offered by the  $NN$  process for studying the interface between hadron and quark dynamics.

In principle, all properties of hadronic processes should be derivable from the fundamental theory of the strong interactions, Quantum Chromodynamics (QCD). However, the mathematical complexities presented by QCD forbids the direct use of this theory for treating strongly interacting processes at low energies. Therefore, in practice one is required to use models with effective degrees

of freedom. In this respect, the use of relativistic quantum field models with baryon and meson degrees of freedom for studying low energy hadronic processes is common practice. In fact, such models have been used for a long time for treating nucleon-nucleon ( $NN$ ) processes, and have been reasonably successful in the description of the empirical data [5,6]. It is therefore natural to expect that such hadronic models are adequate for treating the  $NN$  processes. On the other hand, it is clear that a hadronic description must break down for those observables which receive short-distance contributions, i.e., contributions from distances where quark and gluon degrees of freedom are directly involved. Whereas for those observables that are thought to be insensitive to the short distance physics, such a hadronic approach should be adequate. However, there is one major difficulty one must face when using relativistic quantum field models, namely the problem of renormalization of the ultraviolet divergencies that plague the models. Three different renormalization attitudes are usually followed in the literature: (i) the ultraviolet divergencies are cut off by parameters adjusted phenomenologically, (ii) the model is renormalizable in the sense that it has a finite number of coupling constants that are fixed by a finite number of counter terms necessary to eliminate the ultraviolet divergencies, (iii) the model has an infinite number of coupling constants and the ultraviolet divergencies are absorbed in the redefinition of the coupling constants order by order in the expansion in powers of the momenta involved in the process. Attitude (i) is a pragmatic one; the cutoff is used to eliminate the short distance physics associated

Fellow from CNPq Brazilian Agency. Electronic address: carocha@phys.washington.edu

<sup>y</sup>Electronic address: gkrein@exp.ift.unesp.br

<sup>z</sup>Electronic address: wilets@phys.washington.edu

with the models, since baryons and mesons are composite particles the short distance physics is properly treated once their quark and gluon structure is taken into account. The use of renormalizable models, attitude (ii), is theoretically preferred since the number of parameters is finite and has been proved to be very successful in perturbative calculations of QCD and electroweak processes. Attitude (iii) has been pursued recently in the context of chiral perturbation theory [7,8,9,10,11], and has the potentiality to become useful if higher order calculations, which are required for intermediate to high energy hadronic processes, can be implemented in practice.

The present paper starts with attitude (ii). As said above, one advantage of using renormalizable models is that they are characterized by a finite number of coupling constants and therefore contributions from quantum fluctuations of the fields can be calculated without introducing additional short-distance cutoffs. The insensitivity of low energy observables to the short distance physics associated with the models is obviously crucial for the success of such an approach. In this paper we examine the insensitivity to short distance physics of a renormalizable hadronic model by examining the effects of quantum fluctuations for the nucleon propagator in low energy N scattering. An important question in the process of calculating quantum fluctuations for propagators is the problem of appearance of complex poles, or ghost poles, in the renormalized nucleon and meson propagators. The appearance of ghost poles have long been noted in local relativistic theory [12,14]. The presence of ghost poles in the propagators violates basic theorems of local quantum field theory, and the ghosts are physically unacceptable because they correspond to eigenstates of the system with complex energies and probabilities. In the case of quantum electrodynamics (QED), the complex pole in the photon propagator is known as the Landau ghost. The presence of the Landau ghost is not taken as a serious drawback of QED since the momentum scale at which it appears is far from measurable and, at this scale QED should probably be modified to include other electroweak effects. However, for hadronic models the ghosts are a problem, since they appear in the meson and nucleon propagators at a scale as low as the nucleon mass.

Brown, Puri and Wilets (BPW) [13] calculated the renormalized nucleon propagator in the Hartree-Fock (HF) approximation, which amounts to summing all planar meson diagrams with one nucleon line as shown schematically in Fig. 1 (a). The renormalized propagator was well defined and self-consistent, but contained a pair of ghost poles located approximately 1 GeV on the real and complex axes. BPW have also shown that in the HF approximation the ghosts come from the ultraviolet behavior of the nucleon-meson interaction. This is emphasized by the fact that asymptotically free models appear to be free of ghost poles [15]. Recently, Krein, Nielsen, Puri, and Wilets (KNPW) [16] resumed the study of ghost poles in the nucleon propagator. Following ear-

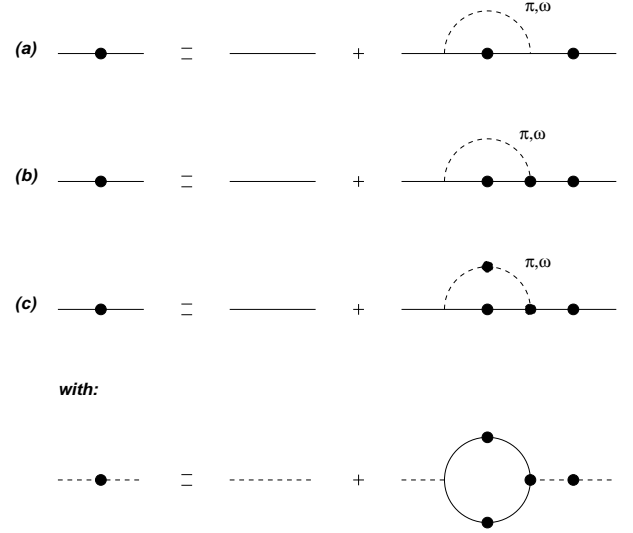


FIG. 1. Diagrammatic representation of the Schwinger-Dyson equations: for the nucleon propagator (a) in the Hartree-Fock approximation and (b) with form-factor dressing of the vertices as in Ref. [16], and (c) for the meson and nucleon propagators as in Ref. [19]. The solid lines refer to nucleons and the dashed lines refer to mesons. A blob indicates nonperturbative quantities.

lier studies by Milana [17] and Allendes and Serot [18], KNPW investigated the effect on the ultraviolet behavior of the interaction by the dressing of the nucleon-meson vertices by means of the neutral vector meson  $\omega$ . The vector-meson dressing of the vertices gives rise to a form factor similar to the Sudakov form factor in QED and has the effect of softening the ultraviolet behavior of the interaction and killing the ghosts. This vertex dressing is shown schematically in Fig. 1 (b). In a more recent paper [19] the coupled SDE's for the nucleon and meson propagators were solved self-consistently in an approximation that goes beyond the Hartree-Fock approximation, see Fig. 1 (c). The main result was that the positions in the complex plane of the ghost poles of both nucleon and meson propagators are rather insensitive to the self-consistency.

The first study of N scattering using the "dressed" nucleon propagator was done by Nutt and Wilets (NW) [20] in the context of HF approximation. NW used a renormalizable hadronic model with pseudoscalar pion-nucleon coupling, including the  $\omega$  meson, to calculate N scattering amplitudes. Using the pole approximation for the nucleon propagator (just the first graph of Fig. 1 (a) after the equal sign), they found the familiar bad result of a zero value for the isospin-even amplitude  $A^{(+)}$ . Besides, the inclusion of just the nucleon pole causes a serious problem in that it produces very large S-wave N amplitudes which leads to an unphysical behavior in the scattering length and in the total cross

section near threshold. Including the nucleon self-energy term, i.e., including the non-delta function part of spectral function, the result becomes  $A^{(+)} = 0.17g^2 = M$  where  $g$  is the pion-nucleon coupling constant and  $M$  is the nucleon mass. Including the ghost poles, i.e., using the entire spectral function of the nucleon propagator, NW found a much better agreement. The result of NW is  $A^{(+)} = 0.99g^2 = M$  for the ghosts alone, and  $A^{(+)} = 0.82g^2 = M$  for the total contribution, while the Adler theorem gives  $A^{(+)} = g^2 = M$  [21,22]. The interpretation of this result is that the role of the ghost pole is to cancel the unphysical behavior of the low-energy observables. The rationale for the NW result was that the ghost poles must be included in the calculations for reasons of consistency, although violating some basic theorems of quantum field theory.

where we have used the abbreviations:

$$M = gv; \quad (10)$$

$$m^2 = \frac{2}{0} + 2v^2; \quad (11)$$

$$m^2 = \frac{2}{0} + 32v^2; \quad (12)$$

In the form of Eq. (8), the nucleon mass is  $M$  and is given by (10), which is the Goldberger-Treiman relation for  $g_A = 1$ ; the pions and the  $\eta$  are no longer degenerate in mass. The value of  $v$  is determined by the condition (6) and the PCAC relation, which gives  $v = f$  at tree level,  $f$  being the pion decay constant. As pointed out by Lee [24], both lagrangians (2) and (8) are completely equivalent. All the Feynman rules derived from this lagrangian are very straightforward and more details can be found on Lee's book.

Next, we discuss the spectral representations of the nucleon propagator and of its inverse. We do not intend to review the subject of spectral representations, we simply make use of the relevant equations for the purposes of the present paper. We refer the reader to Refs. [25,26,27]. The nucleon propagator is defined as

$$G(x^0, x) = i \langle 0 | T [ \psi(x^0, x) \bar{\psi}(0) ] | 0 \rangle; \quad (13)$$

where  $|0\rangle$  represents the physical vacuum state. Following the BPW approach, the Kallen-Lehmann representation for the Fourier transform  $G(p)$  of  $G(x^0, x)$  can be written as

$$G(p) = \int_0^{\infty} d\phi \frac{A(\phi)}{\phi + i}; \quad (14)$$

where  $A(\phi)$  is the spectral function. It represents the probability that a state of mass  $\phi$  is created by  $\psi$  or  $\bar{\psi}$ , and as such it must be non-negative. Negative corresponds to states with opposite parity to the nucleon.

Defining the projection operators

$$P(p) = \frac{1}{2} (1 + \frac{\not{p}}{w_p}); \quad (15)$$

where

$$w_p = \sqrt{p^2} = \begin{cases} p & \text{if } p^2 > 0 \\ i & \text{if } p^2 < 0; \end{cases} \quad (16)$$

$G(p)$  can be rewritten conveniently as

$$G(p) = P_+(p) \tilde{G}(w_p + i) + P_-(p) \tilde{G}(w_p - i); \quad (17)$$

where  $\tilde{G}(z)$  is given by the dispersion integral

$$\tilde{G}(z) = \int_0^{\infty} d\phi \frac{A(\phi)}{z - \phi}; \quad (18)$$

The inverse of the propagator can also be written in terms of the projection operators  $P_{\pm}(p)$  as

$$G^{-1}(p) = P_+(p) \tilde{G}^{-1}(w_p + i) + P_-(p) \tilde{G}^{-1}(w_p - i); \quad (19)$$

The spectral representation for  $\tilde{G}^{-1}(z)$  is written as,

$$\begin{aligned} \tilde{G}^{-1}(z) &= z - M_0 - \tilde{\Sigma}(z) \\ &= z - M_0 - \int_0^{\infty} d\phi \frac{T(\phi)}{z - \phi}; \end{aligned} \quad (20)$$

The function  $\tilde{\Sigma}(z)$  is related to the nucleon self-energy  $\Sigma(q)$  (see Eq. (28)) by the projection operators  $P_{\pm}(q)$  as in Eq. (19).

Since  $A(\phi)$  is supposed to be non-negative,  $\tilde{G}(z)$  and  $\tilde{G}^{-1}(z)$  can have no poles or zeros on the real axis. This is known as the Herglotz property [13]. In general, the integral in Eq. (20) needs renormalization. The usual mass and wave-function renormalizations are performed by imposing the condition that the renormalized propagator has a pole at the physical nucleon mass  $M$ , with unit residue. This implies that the renormalized propagator  $\tilde{G}_R(z)$ , defined as

$$\tilde{G}_R(z) = \tilde{G}(z) Z_2; \quad (21)$$

is given by the following expression:

$$\tilde{G}_R(z) = \int_0^{\infty} d\phi \frac{A_R(\phi)}{z - \phi}; \quad (22)$$

and the inverse of the propagator is given by

$$\begin{aligned} \tilde{G}_R^{-1}(z) &= (z - M) \\ &= (z - M) - \int_0^{\infty} d\phi \frac{T_R(\phi)}{(\phi - M)^2 (z - \phi)}; \end{aligned} \quad (23)$$

In the above expressions,  $A_R(\phi) = A(\phi) Z_2$  and  $T_R(\phi) = Z_2 T(\phi)$ . In terms of renormalized quantities,  $Z_2$  can be written as

$$Z_2 = 1 - \int_0^{\infty} d\phi \frac{T_R(\phi)}{(\phi - M)^2}; \quad (24)$$

or

$$Z_2 = \int_0^{\infty} d\phi A_R(\phi) : \quad (25)$$

The spectral functions  $A_R(\phi)$  and  $T_R(\phi)$  are related by

$$A_R(\phi) = (\phi - M) + j \tilde{G}_R^{-1}((1+i)\phi) j^2 T_R(\phi) \quad (26)$$

$$(\phi - M) + A_R(\phi) : \quad (27)$$

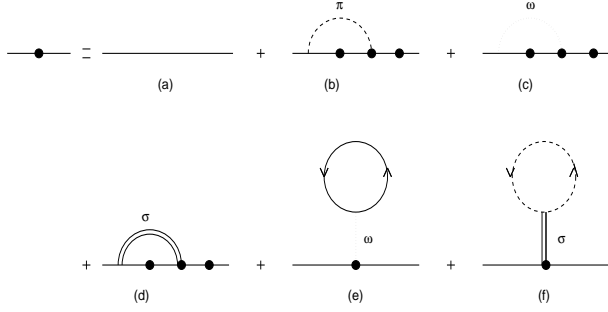


FIG. 2. Diagrammatic representation of SDE. The tadpole diagrams do not contribute because they drop out in the renormalization process.

### B. Schwinger-Dyson equation for the nucleon propagator

In this section we calculate the "dressed" nucleon propagator with its self-energy given by contributions of  $\pi$ ,  $\omega$ , and  $\sigma$  mesons. The Schwinger-Dyson equation (SDE) for the nucleon propagator in momentum space is given by the following expressions

$$G(p) = G^{(0)}(p) + G^{(0)}(p) \Sigma(p) G(p); \quad (28)$$

where

$$\begin{aligned} \Sigma(p) = & ig_0^2 \int \frac{d^4 q}{(2\pi)^4} \gamma_5 D(q^2) G(p-q) \gamma_5 (\not{p}-q; p; q) \\ & + ig_1^2 \int \frac{d^4 q}{(2\pi)^4} D_1(q^2) G(p-q) (\not{p}-q; p; q) \\ & + ig_0^2 \int \frac{d^4 q}{(2\pi)^4} D(q^2) G(p-q) S(p-q; p; q); \quad (29) \end{aligned}$$

is the nucleon self-energy, shown schematically in Fig. 2. In Eq. (29),  $D$ ,  $D_1$ , and  $D_2$  are the  $\pi$ ,  $\omega$ , and  $\sigma$  propagators and  $\gamma_5 (\not{p}-q; p; q)$ ,  $(\not{p}-q; p; q)$ , and  $S(p-q; p; q)$  are respectively the pion-nucleon, omega-nucleon, and sigma-nucleon vertex functions. The tadpoles in Fig. 2 do not contribute to the nucleon propagator, since they drop out in the renormalization procedure. The Hartree-Fock (HF) approximation amounts to using the noninteracting meson propagators and bare vertices  $\gamma_5 (\not{p}-q; p; q) = \gamma_5 \not{p}$ ,  $(\not{p}-q; p; q) = \not{p}$ , and  $S(p-q; p; q) = 1$  in Eq. (29). In order to regulate the ultraviolet behavior of the interaction and study the role of a ghost-free self-consistent propagator, we consider simplified vertex functions that are written as:

$$\gamma_5 (\not{p}; p_2; q) = \gamma_5 F_5(p_1; p_2; q) \quad (30)$$

$$(\not{p}; p_2; q) = F_V(p_1; p_2; q) \quad (31)$$

$$S(p; p_2; q) = F_S(p_1; p_2; q); \quad (32)$$

where  $F_5(p_1; p_2; q)$ ,  $F_V(p_1; p_2; q)$ , and  $F_S(p_1; p_2; q)$  are scalar functions. Substituting Eqs. (30-32) and the spectral representations for  $G(p)$  in the integral for  $\Sigma(p)$ , Eq. (29), and using the projection operators  $P_{\pm}(p)$ , one obtains:

$$T_R(\omega) = \int_0^{\omega+1} d\omega K(\omega; \omega) A_R(\omega); \quad (33)$$

where  $K(\omega; \omega)$  is the scattering kernel given by

$$\begin{aligned} K(\omega; \omega) = & K(\omega; \omega; m^2) \\ & + 2K_1(\omega; \omega; m^2) + K_2(\omega; \omega; m^2); \quad (34) \end{aligned}$$

with  $K(\omega; \omega; m^2)$ ,  $K_1(\omega; \omega; m^2)$ , and  $K_2(\omega; \omega; m^2)$  being respectively the  $\pi$ ,  $\omega$ , and  $\sigma$  contributions, given by

$$\begin{aligned} K(\omega; \omega; m^2) = & F_5(\omega; \omega; m^2) \frac{g^2}{4} \frac{1}{2j j^3} \\ & \int_0^{\omega+1} d\omega' \frac{2\omega'^2(\omega'^2 + m^2) + (\omega'^2 - m^2)^2}{(\omega'^2 - m^2)^2} \frac{1}{(j^0 j + m^2)^2}; \quad (35) \end{aligned}$$

$$\begin{aligned} K_1(\omega; \omega; m^2) = & F_V(\omega; \omega; m^2) \frac{g_1^2}{4} \frac{1}{2j j^3} \\ & \int_0^{\omega+1} d\omega' \frac{2\omega'^2(\omega'^2 + m^2) + (\omega'^2 - m^2)^2}{(\omega'^2 - m^2)^2} \frac{1}{(j^0 j + m^2)^2}; \quad (36) \end{aligned}$$

and

$$\begin{aligned} K_2(\omega; \omega; m^2) = & F_S(\omega; \omega; m^2) \frac{g^2}{4} \frac{1}{2j j^3} \\ & \int_0^{\omega+1} d\omega' \frac{2\omega'^2(\omega'^2 + m^2) + (\omega'^2 - m^2)^2}{(\omega'^2 - m^2)^2} \frac{1}{(j^0 j + m^2)^2}; \quad (37) \end{aligned}$$

In the above equations,  $g$  and  $g_1$  are the renormalized coupling constants, defined as  $g = Z_2 g_0$  and  $g_1 = Z_2 g_{01}$ .

### C. Ghost poles

Next we discuss the numerical solution of the SDE. The problem consists in solving for the spectral function  $A_R(\omega)$ . The equations involved are Eqs. (23), (27) and (33)-(37). These represent a set of coupled nonlinear integrodifferential equations which are solved by iteration [13,16].

Initially, we consider bare vertices:  $F_5(p_1; p_2; q) = F_V(p_1; p_2; q) = F_S(p_1; p_2; q) = 1$ , and study the convergence properties of the SDE for the nucleon self-energy. The new aspect here is the presence of the chiral partner

of the pion, the  $\pi$ . We consider the following cases: (a)  $\pi$  meson only, (b)  $\pi + \sigma$  mesons, and (c)  $\pi + \sigma + \omega$  mesons. We use the following values for the coupling constants:

$$\frac{g^2}{4} = \frac{g^2}{4} \quad \frac{g^2}{4} = 14.6 \quad (38)$$

$$\frac{g_1^2}{4} = 6.36; \quad (39)$$

where we wrote explicitly that the value of the sigma-nucleon coupling constant is equal to the pion-nucleon one, as required by the linear realization of chiral symmetry.

The first fact we observed in solving the SDE was that the introduction of the chiral partner of the pion does not remove the ghost poles. As the mass of the  $\sigma$  meson remains a point of debate, we varied  $m_\sigma$  over a wide range. The solutions of SDE converge quickly in the studied range, 500  $m_\sigma$  1500 MeV. For the case of using the  $\pi$  only, the convergence is more difficult to achieve for  $m_\sigma$  between 550 and 770 MeV, but it was obtained by using a small convergence factor at each iteration. However, this case is of little interest for NN scattering, since pions are always present. The converged spectral functions  $A_R(\kappa)$  are shown in Fig. 3. We used the following values for the meson masses:

$$m_\pi = 138.03 \text{ MeV}; \quad (40)$$

$$m_\sigma = 783 \text{ MeV}; \quad (41)$$

$$m_\omega = 550; 770; 980 \text{ MeV and } m_\rho = 1; \quad (42)$$

The reason for using this particular set of masses is the following:  $m_\pi = 550 \text{ MeV}$  is the value commonly used in the One Boson Exchange Potentials (OBE) [5,6];  $m_\sigma = 770 \text{ MeV}$  is the value used by Serot and Walecka [28] in the calculations of nuclear matter properties using the chiral linear sigma model;  $m_\omega = 980 \text{ MeV}$  is the first scalar meson in the mesons table,  $f_0$ , and the limit  $m_\rho \rightarrow 1$  supplies the connection between the linear realization of chiral symmetry and the minimal chiral model of the non-linear realization of chiral symmetry in NN system [29]. Recently, Tomqvist and Roos [30] claimed that the sigma meson really exists, with a mass of 860 MeV and an extremely broad width of 880 MeV. Although this fact is receiving great attention lately, a final word of existence in this mass region remains to be stated.

Fig. 3-top presents the nucleon dressed by the  $\pi + \sigma + \omega$  mesons, for  $m_\sigma = 550 \text{ MeV}$  and  $m_\rho = 1$ . We note that  $A_R(\kappa)$  for positive  $\kappa$  is much larger than for negative  $\kappa$ , it increases as the mass increases, and becomes equal to the  $\pi + \sigma$  case (NW's study) in the limit  $m_\rho \rightarrow 1$ . Recall that for  $m_\rho \rightarrow 1$  the  $\rho$  meson does not contribute to  $A_R(\kappa)$ . Starting from  $m_\rho \rightarrow 1$  and going down, one finds that the presence of the  $\rho$  meson modifies drastically the spectral function for positive  $\kappa$ , decreasing the main peak and creating a second resonance peak; for negative  $\kappa$ , the changes are very small. The zeros of  $A_R(\kappa)$

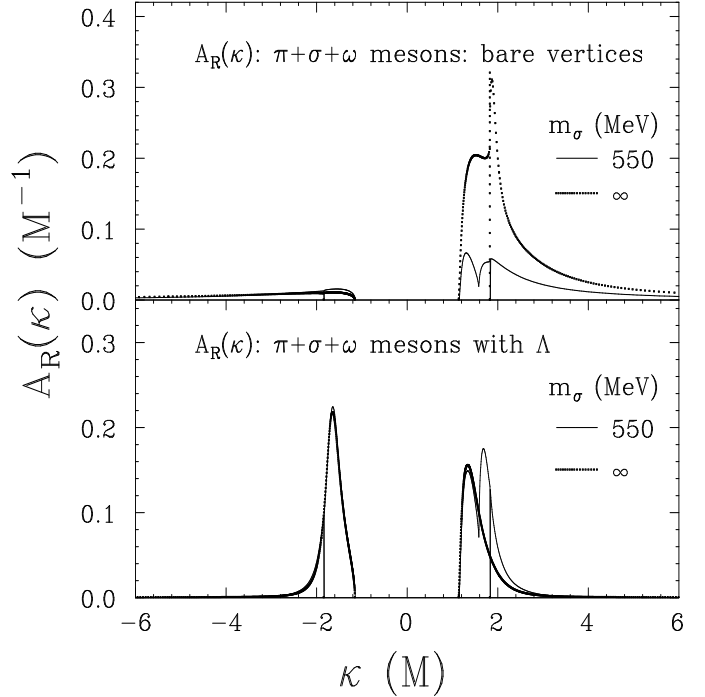


FIG. 3. Top: plot of  $A_R(\kappa)$  as a function of  $\kappa$  for nucleon self-energy due to  $\pi + \sigma + \omega$  mesons with bare nucleon vertices. Bottom: the same study for the same system but with vertices dressed by form factors. For the other masses, the curves are between these two curves.

TABLE I. Ghost poles positions and residues for  $\pi + \sigma + \omega$  dressing with different masses.

Process	Pole position (units of $M$ )	Pole residue (dimensionless)
$\pi + \sigma + \omega$ (550)	0.2624 i0.4402	0.6208 i1.1281
$\pi + \sigma + \omega$ (770)	0.4043 i0.7648	0.6317 i0.5616
$\pi + \sigma + \omega$ (980)	0.5147 i0.9147	0.6431 i0.4143
$\pi + \sigma + \omega$ (1)	1.1058 i1.1337	0.7410 i0.1788

at  $\kappa = \pm(M + m_\rho)$  shown in the figure are due to the discontinuity of the  $\rho$  kernel, Eq. (36), at these points as explained in Ref. [16]. The  $\pi + \sigma$  system revealed minor differences, since the contribution of the  $\rho$  meson is small and come from the region near  $\kappa = \pm(M + m_\rho)$ . The position of the ghost poles and the value of their residues are shown in Tab. I, where one sees that the real part of the complex pole position ( $P_R$ ) increases with the mass. At the usual  $m_\rho = 550 \text{ MeV}$ ,  $P_R$  is a little below  $2m_\pi$ , which means that the inclusion of the  $\rho$  meson in the nucleon self-energy brings down the position of the ghosts from 1 GeV to near 300 MeV.

Next we consider vertex form factors. In principle one can use the corresponding Sudakov form factors, as in Ref. [16]. However, since the Sudakov form factor is known exactly in the ultraviolet only, one has to interpolate it in some way down to the infrared or simply

parameterize its infrared behavior. However, since for our purposes here of killing the ghosts the infrared behavior is not relevant, we prefer to simplify matters and use parameterized form factors, which implies that we can not make any conclusion involving chiral symmetry in these approach, since this phenomenological vertex dressing has no connection with chiral symmetry.

For general  $\omega$ -shell legs, we use the factorized form of Pearce and Jennings [2]; for a vertex with four-momenta  $p, p, p, p$ , the form factor is

$$F = F(p^2)F(p^2)F(p^2) : \quad (43)$$

For mesons we adopt the expressions by Gross, Van Orden and Holinde [31]

$$F_m(q^2) = \frac{1 + \frac{1}{(1 - \frac{q^2}{m^2})^2}}{1 + \frac{1}{(1 - \frac{q^2}{m^2})^2}} \quad (44)$$

where  $m$  is the meson cutoff mass. For the nucleon legs we adopt the expressions by Gross and Surya [3]

$$F_B(p^2) = \frac{(\frac{2}{B} - \frac{m_B^2}{p^2})^2}{(\frac{2}{B} - \frac{m_B^2}{p^2})^2 + (m_B^2 - p^2)^2} \quad (45)$$

where  $B$  is the nucleon cutoff mass. Both meson and nucleon form factors have the correct on-shell limit, equal to unity.

At this point it is perhaps convenient to call attention that we use form factors for regulating the ultraviolet with the only aim of studying the role of a ghost-free propagator in  $N$  scattering. In principle, the form factors are calculable within the model by means of vertex corrections. In particular, such vertex corrections must satisfy Ward-Takahashi identities that follow from chiral symmetry, and of course our form factors  $F_S$  and  $F_V$ , Eq. (44), do not satisfy such identities. This interesting subject is intended to be pursued in a future work.

The cutoff values  $B$  and  $m$  are constrained to kill the ghost poles and give the best fit to the scattering lengths. There is a critical value  $c$  such that for  $c < c$  the ghosts disappear [16]. The values for  $c$  for all systems studied in this paper are shown in the second column of Tab. II. Note that the form factors corresponding to the meson legs do not contribute in the SDE (see Eqs. (35-37)). One observes that  $B < c$ . The constraints related to the scattering lengths are discussed in Sec. III C.

Fig. 3-bottom presents the case  $\pi + \pi$ , with form factors at each vertex. We use  $B = 1330$  MeV. The shape of  $A_R(s)$  depends strongly on the  $m$  mass for  $m > 0$  only. One sees that the second peak is mainly due to the  $\omega$  meson, it decreases as the  $m$  mass increases and disappears in the limit  $m \rightarrow 1$ . The interesting effect due to the form factors is that the spectral function for  $c < 0$  becomes very large as compared to the case of bare vertices. This will have serious consequences for the observables of  $N$  scattering. The position of the peaks

TABLE II. Critical values of the nucleon cutoff (in MeV), position of the peaks in  $A_R(s)$  (in MeV), and the integral of  $A_R(s)$  over  $s$ .

System	$c$	1 <sup>st</sup> Peak	2 <sup>nd</sup> Peak	3 <sup>rd</sup> Peak	Area
only	2085	-1541	1263	-	0.1923
$\pi$ only	9550	-1807	1777	-	-0.0008
$\pi + \pi$	1815	-1536	1268	-	0.1919
(550)	2650	-1717	1569	-	0.0259
(770)	3477	-1967	1778	-	0.0045
(980)	4523	-2208	1997	-	0.0011
(1581)	5390	-2913	2628	-	0.0001
$\pi + (550)$	1817	-1545	1257	1581	0.2328
$\pi + (770)$	1951	-1541	1262	1751	0.2002
$\pi + (980)$	2026	-1541	1263	1933	0.1947
$\pi + (1)$	2071	-1541	1265	-	0.1923
$\pi + \pi + (550)$	1822	-1541	1257	1581	0.2324
$\pi + \pi + (770)$	1958	-1536	1263	1723	0.1998
$\pi + \pi + (980)$	2037	-1536	1268	1940	0.1943
$\pi + \pi + (1)$	2085	-1541	1263	-	0.1923

in the spectral function for the different cases studied are presented in the third to fifth columns of Tab. II.

The contribution of each meson to the nucleon self-energy can be estimated by the integral over the spectral function  $A_R(s)$ . The integral is related to the renormalization constant  $Z_2$  as indicated in Eq. (25). This is shown in the last column of Tab. II. One notices that the pion gives the highest contribution, followed by the lightest sigma meson (550 MeV) and the omega meson. This indicates that the dressing of the nucleon is mainly due to the pion.

### III. N SCATTERING AND GHOST POLES

#### A. Introduction

The simplest field-theoretical model for  $N$  scattering is the summation of Feynman diagrams in tree approximation [4]. Such a model can involve only pions and nucleons [7] or it may be augmented by hadronic resonances like the  $\omega$  and the  $\rho$  in the baryonic sector or the  $\pi$ , and others mesons in the mesonic sector [4]. The differences between these models come from the inclusion or not of chiral symmetry and how far one desires to reproduce the experimental data. In Born approximation, when using pions and nucleons only, the lowest order contribution is the sum of just two graphs, as shown in Figs. 4(a,b). As is well known, these first two contributions give bad results for isoscalar observables.

According to the  $\omega$ -linear lagrangian, Eq. (8), the  $N$  coupling is pseudoscalar (PS) and two new couplings appear,  $NN$  and  $\pi\pi$ . The lowest order tree diagrams contain one more diagram, as shown in Fig. 4(c), which inclusion led to an almost perfect fit to the value of the isospin-even amplitude  $A^{(+)}$  at threshold. This is one of

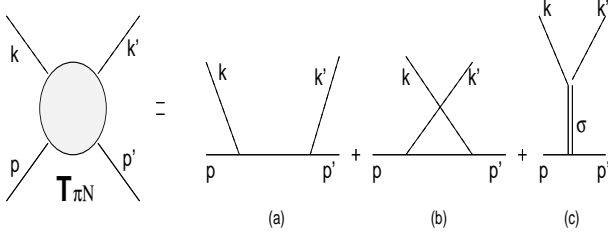


FIG. 4. (a), (b) Order  $g^2$  contributions involving only pions and nucleons. (c) Scalar meson contribution.

the classical examples of the importance of chiral symmetry in hadronic interactions.

In the 70's, Nutt and Willets [20] found the result that the threshold value of  $A^{(+)}$  could be explained by introducing quantum fluctuations in the nucleon propagator. NW used the BPW formalism to solve the SDE equation for the nucleon propagator. As discussed in the previous section, the renormalized nucleon propagator is well defined and self-consistent, but contains a pair of complex ghost poles. In the Sec. III C we re-investigate this result on the light of dressed nucleon propagators free of ghosts.

#### B. Bare nucleons

At lowest order (tree level) the scattering amplitude for  $(k)N(p) \rightarrow (k')N(p')$ , where  $p$  and  $p'$  ( $k$  and  $k'$ ) are the nucleon (pion) four-momentum, and  $\alpha$  and  $\alpha'$  the isospin labels, can be described by a model involving the processes shown in Fig. 4, plus the contribution of  $\Delta$  and  $\Delta^*$  resonances. Such a model provides a good description of data from threshold until pion energies up to 350 MeV [32], 400 MeV [2], and 600 MeV [3]. The  $\Delta$ -term is needed for the implementation of chiral symmetry in a linear way. At tree level, the  $\Delta$ -exchange can be understood as representing a function that, in the context of current algebra, comes from the equal-time commutator of an axial current and its divergence. Usually this contribution is represented by a parameterized form [33,34].

The  $N$  amplitude  $T_N$  can be parameterized as [20]

$$T_N = u(p^0) [A^{(+)} + \frac{1}{2} (\mathbb{K} + \mathbb{K}^0) B^{(+)}]_{ab} + A^{(-)} + \frac{1}{2} (\mathbb{K} + \mathbb{K}^0) B^{(-)}]_{i_b a c c} u(p); \quad (46)$$

where  $A^{(+)}$  and  $B^{(+)}$  are Lorentz invariant functions that contain the dynamics of the model. Let us first examine the nucleon pole and scalar exchange. For the diagrams shown in Fig. 4 we get

$$A^{+}(s; t; u) = \frac{g^2}{M} \frac{1}{1 - \frac{(m - M)^2}{t - m^2}}; \quad (47)$$

$$A^{-}(s; t; u) = 0; \quad (48)$$

$$B^{+}(s; t; u) = g^2 \left[ \frac{1}{s - M^2} - \frac{1}{u - M^2} \right]; \quad (49)$$

$$B^{-}(s; t; u) = g^2 \left[ \frac{1}{s - M^2} + \frac{1}{u - M^2} \right]; \quad (50)$$

$B^{+}$  and  $B^{-}$  receive contributions from nucleon intermediate states, and  $A^{+}$  from  $\Delta$  exchange. If one takes the limit  $m \rightarrow 0$  for a fixed  $t$ , the  $A^{+}$  result is

$$A^{+}(s; t; u) = \frac{g^2}{M}; \quad (51)$$

This limit corresponds to a contact scalar interaction of two pions with the nucleon, and is the exact result of Adler theorem [21,22]. It is worth noting that the isospin even exchange term  $(A^{+} + m B^{+})$  vanishes in the zero four-momentum transfer limit at threshold ( $s = M^2 + m^2$ ;  $t = 0$ ;  $u = M^2 - m^2$ ), if we neglect terms proportional to  $m^2/M^2$ .

Next we calculate the scattering length  $a$ . It is given in terms of the  $T$ -matrix as:

$$a = \frac{1}{8(M + m)} \mathcal{T}^i_{i, \text{threshold}}; \quad (52)$$

where  $\mathcal{T}^i_{i, \text{threshold}}$  is the scattering amplitude  $T$  calculated at threshold ( $p = M$ ).  $T$  is related to the differential cross section as

$$\frac{d}{d} = \frac{1}{(8W)^2} \mathcal{T}^i f^2; \quad (53)$$

where  $W$  is the total invariant mass of the final state. In deriving Eq. (52) the cross section was approximated by the area of a black sphere of radius  $a$ , which is a good approximation at very low energies. In terms of the invariants  $A^{(+)}$  and  $B^{(+)}$ ,  $a$  can be written as (in the c.m. frame):

$$a = \frac{1}{4(1 + m/M)} [A^{(+)} + m B^{(+)}]; \quad (54)$$

The experimental values for the scattering lengths are [32]

$$a^{+} = (0.021 \pm 0.021) \text{ fm} \\ a^{-} = 0.139 \pm 0.004 \text{ fm} \quad (55) \\ \quad \quad \quad 0.010 \text{ fm}$$

In Tab. III we show the results using the delta function piece of the nucleon propagator with and without chiral symmetry (CS). In obtaining these results no form-factors at the meson-nucleon vertices were used. One sees that inclusion of chiral symmetry improves the results for the scattering lengths in the isoscalar channel. This is due to a strong cancellation of the nucleon pole



TABLE III. Scattering lengths with and without chiral symmetry at the tree level, using bare nucleon propagator and bare vertices. Chiral symmetry is indicated by C.S. The experimental values are given in Eq. (55).

Process	$A^+$ ( $g^2=M$ )	$A$ ( $g^2=M$ )	$m \rightarrow 0$ ( $g^2=M$ )	$m \rightarrow 0$ ( $g^2=M$ )	$a^+$ (fm)	$a$ (fm)
Fig. 4 (a+b) - no C.S.	0	0	-1.005433	0.07391	-2.6896	0.1977
Fig. 4 (a+b+c) - with C.S.						
$m = 550$ MeV	0.93700	0	-1.005433	0.07391	-0.1830	0.1977
$m = 770$ MeV	0.96786	0	-1.005433	0.07931	-0.1005	0.1977
$m = 980$ MeV	0.98020	0	-1.005433	0.07931	-0.0676	0.1977
$m \rightarrow 0$	1.0000	0	-1.005433	0.07931	-0.0145	0.1977

( $B^+$ ) with the exchange ( $A^+$ ). This cancellation is exact if we take the limit  $m \rightarrow 0$  and  $m^2=M^2 \rightarrow 0$ . The magnitude of the scattering length  $a^+$  is almost zero, it is proportional to  $m^2=M^2$ . In the chiral limit,  $m \rightarrow 0$ , the scattering lengths are zero. This is a property of the linear  $\sigma$  model Lagrangian at the tree level.

#### C. Dressed nucleons

The graphs that contribute to the  $N$  scattering are given in Fig. 4, where the nucleon propagators are now "dressed" by the  $\pi$  mesons. The new contributions, as we compared to the NW's work, are the inclusion of the scalar meson both in t channel scattering and in the nucleon self energy. The contribution of the non-delta part of the spectral function, defined in Eq. (27), to the functions  $A$ ,  $B$  is given by:

$$A(s;t;u) = g^2 \int_0^1 dA(\lambda) \left( \frac{1}{s-\lambda^2} - \frac{1}{u-\lambda^2} \right) \quad (56)$$

$$B(s;t;u) = g^2 \int_0^1 dA(\lambda) \frac{1}{s-\lambda^2} - \frac{1}{u-\lambda^2} \quad (57)$$

The total contribution for  $A$  and  $B$  is the sum of three parts coming from: (a) the delta function part of  $A(\lambda)$ , given in Eqs. (47-50), (b) the self-energy given by Eqs. (56-57), and (c) the ghost poles. The contribution from the ghost poles is given by:

$$A_g(s;t;u) = g^2 \sum_c A_c(\lambda_c) \left( \frac{1}{s-\lambda_c^2} - \frac{1}{u-\lambda_c^2} \right) \quad (58)$$

$$B_g(s;t;u) = g^2 \sum_c A_c \frac{1}{s-\lambda_c^2} - \frac{1}{u-\lambda_c^2}; \quad (59)$$

where the sum is over  $(\lambda_c; A_c)$  and its complex conjugate  $(\lambda_c^*; A_c^*)$ .

Tab. IV shows the results for  $A^+$  and the scattering lengths  $a$  for two cases:  $m = 138.03$  MeV and the chiral limit  $m = 0$ . The low-energy theorems impose in the second case that  $A^+ = 1$  (in  $g^2=M$  units) and  $a = 0$ . All results are obtained with no form factors in either the Schwinger-Dyson equation nor in the scattering amplitudes.

The results for the scattering lengths should be compared with the experimental values given in Eq. (55), and with the predictions of the low-energy theorems. The  $\pi$  system was also studied and the results are very similar to the  $\pi$  system. All the contributions for the observable  $a^+$  are very far from the experimental result; the results of NW are given in Sum (E); their results for the chiral limit  $m = 0$  are correct within 13% for  $A^+$  but they are very large for the  $a^+$  observable. Therefore if we examine the low-energy observables, the ghost poles play no longer a special role. Our conclusion here is that, as the sum of ghosts plus  $\pi$  contributions exceeds by a large amount the experimental values of the  $a^+$  scattering length, the ghosts are a product of the chosen approximations, which reveal to be not appropriate at the loop order.

In order to get rid of the ghosts we change our study to a more phenomenological point of view. Using form factors, we investigate the role of a ghost free nucleon propagator. One needs first to recalculate the nucleon pole contribution plus exchange term using one form factor for each  $\phi$ -shell line at threshold. The sum of all the contributions depends on two free parameters:  $B$  and  $m$ . The last affects the exchange while the former contributes to the

TABLE IV . Results for observables using dressed nucleon propagators: (a)  $m_\pi = 138.08$  MeV and (b) the chiral limit  $m_\pi \rightarrow 0$ . No form factors are used.

Contribution	(a) $m_\pi = 138.08$ MeV			(b) $m_\pi = 0$		
	$A^+$ ( $g^2/M$ )	$a^+$ (fm)	$a$ (fm)	$A^+$ ( $g^2/M$ )	$a^+$ (fm)	$a$ (fm)
1) $+$ (550) $+$ ! : $A_R$ ( )	0.0197	0.0773	0.1108	0.0202	0.0619	0
2) $+$ (550) $+$ ! : ghosts	-0.5894	-1.9462	1.8702	-0.7717	-2.3679	0
3) $+$ (550) $+$ ! : Tree diagrs.	0.9370	-0.1830	0.1977	1.0	0	0
Sum (A) : 1 + 2 + 3	0.3673	-2.0520	2.1790	0.2484	-2.3606	0
4) $+$ (770) $+$ ! : $A_R$ ( )	-0.0061	0.0148	0.0995	-0.0202	-0.0619	0
5) $+$ (770) $+$ ! : ghosts	0.0358	-0.0656	0.7324	-0.1197	-0.3671	0
6) $+$ (770) $+$ ! : Tree diagrs.	0.9679	-0.1005	0.1977	1.0	0	0
Sum (B) : 4 + 5 + 6	0.9976	-0.1514	1.0296	0.8602	-0.4290	0
7) $+$ (980) $+$ ! : $A_R$ ( )	-0.0291	-0.0424	0.0949	-0.0521	-0.1600	0
8) $+$ (980) $+$ ! : ghosts	0.3227	0.7724	0.3677	0.2222	0.6818	0
9) $+$ (980) $+$ ! : Tree diagrs.	0.9802	-0.0676	0.1977	1.0	0	0
Sum (C) : 7 + 8 + 9	1.2737	0.6625	0.6602	1.1701	0.5218	0
10) $+$ (1 ) $+$ ! : $A_R$ ( )	-0.1659	-0.3935	0.0891	-0.2067	-0.6342	0
11) $+$ (1 ) $+$ ! : ghosts	0.9906	2.6735	-0.0821	1.0839	0.9314	0
12) $+$ (1 ) $+$ ! : Tree diagrs.	1.0	-0.01453	0.1977	1.0	0	0
Sum (D) : 10 + 11 + 12	1.8247	2.2654	0.2074	1.8772	2.6917	0
13) NW 's work : $+$ ! : $-A_R$ ( )	-0.1659	-0.3935	0.0891	-0.2067	-0.6342	0
14) NW 's work : $+$ ! : ghosts	0.9906	2.6735	-0.0821	1.0839	3.3259	0
15) NW 's work : $+$ ! : Tree diagrs.	0	-2.6896	0.1977	0	-3.0684	0
Sum (E) : 13 + 14 + 15: NW 's work	0.8247	-0.4097	0.2047	0.8772	-0.3767	0

TABLE V . Values of  $m_\pi$  adjusted to reproduce the scattering length  $a^+$  for  $+$  and  $+$   $+$  ! dressings at different masses.

Process masses (MeV)	$+$ system		$+$ $+$ ! system	
	$m_\pi$	$m_\pi = m_\pi$	$m_\pi$	$m_\pi = m_\pi$
$m_\pi = 550$	822.2825	0.66887	821.4860	0.66952
$m_\pi = 770$	1145.079	0.67244	1143.978	0.67309
$m_\pi = 980$	1455.984	0.67308	1454.585	0.67373
$m_\pi \rightarrow 1$	-	0.67338	-	0.67403

nucleon pole and to the nucleon self-energy. As mentioned before, the ghosts disappear for a  $m_\pi$  less than a critical value  $m_c$ .

To fix the values for the cutoff parameters, we first choose a set of  $(m_\pi; m_B)$  values such as to reproduce the value  $a^+ = 0$  for  $m_\pi = 0$ . Therefore, we get a relation between the cutoffs. However, this does not uniquely determine their values. To choose one particular pair of cutoff values, we examined the results for  $a^+$  when  $m_\pi = 138.03$  MeV. It is possible to adjust  $m_\pi$  and  $m_B$  such that all the different nucleon dressings give the correct chiral limit  $a^+ \rightarrow 0$  when  $m_\pi = 0$ ; but only with  $m_B$  approximately 1330 MeV one obtains the correct small and negative result for  $a^+$  when  $m_\pi = 138.03$  MeV. Tab. V shows the values for  $m_\pi$  for  $+$  and  $+$   $+$  ! dressings and different masses. There is one delicate point here, namely the value for  $m_\pi$  when  $m_\pi \rightarrow 1$ . We handle this by making these two quantities go to infinity at the same time, keeping the ratio between them constant to preserve the chiral limit  $a^+ = 0$  when  $m_\pi = 0$ . Our main result here is that  $m_\pi = m_\pi = 0.67$  in order to reproduce the results for  $a^+$  at threshold and at the chiral limit. In doing this, we are constructing a phenomenological model which respects the low-energy theorems in  $NN$  scattering. It is clear also that we can not make any statement about chiral symmetry, since the phenomenological form factors violate the chiral Ward-Takahashi identities.

Tab. VI presents the results for the observables for  $m_\pi = 138.03$  MeV. All cases studied have the correct chiral limit  $A^+ = g^2/M$  and  $a = 0$  for  $m_\pi = 0$ . The results for the case  $+$  are not shown since they are similar to the ones for the  $+$   $+$   $+$  case.

Observable  $A^+$  receives contributions mainly from (a) the  $\pi$ -exchange, Fig. 4 (c), which depends directly on  $m_\pi$ , and (b) from the nucleon self-energy  $A_R$  ( ), which is weakly dependent on  $m_B$  and is almost independent from the mass. The results show that  $\pi$  exchange and the self-energy contribution  $A_R$  ( ) contribute approximately 50% each.

The results for  $a^+$  depend on the sum of  $A^+$  and  $B^+$ . Observable  $B^+$  receives contributions from the nucleon

TABLE VI. Same as in TABLE IV, but using form factors.

Contribution	$A^+$ $g^2=M$	$m_B$ $g^2=M$	$A$ $g^2=M$	$m_B$ $g^2=M$	$a^+$ (fm)	$a$ (fm)
1) + (550) + !: $A_R(\cdot)$	0.3744	0.0249	0.1335	0.0644	1.06820	0.5292
2) + (550) + !: Tree diags.	0.3986	-0.8335	0	0.0613	-1.16336	0.1639
Sum (A): 1 + 2	0.7730	-0.8084	0.1335	0.1267	-0.09516	0.6931
3) + (770) + !: $A_R(\cdot)$	0.3811	0.0249	0.1329	0.0605	1.08513	0.5173
4) + (770) + !: Tree diags.	0.4084	-0.8335	0	0.0613	-1.13713	0.1639
Sum (B): 3 + 4	0.7895	-0.8089	0.1329	0.1218	-0.05200	0.6812
5) + (980) + !: $A_R(\cdot)$	0.3821	0.0246	0.1327	0.06001	1.08771	0.5155
6) + (980) + !: Tree diags.	0.4130	-0.8335	0	0.0613	-1.12486	0.1639
Sum (C): 5 + 6	0.7951	-0.8089	0.1327	0.1213	-0.03715	0.6794
7) + (1) + !: $A_R(\cdot)$	0.3815	0.0246	0.1329	0.0601	1.08640	0.5163
8) + (1) + !: Tree diags.	0.4211	-0.8335	0	0.0613	-1.10326	0.1639
Sum (D): 7 + 8	0.8026	-0.8089	0.1329	0.1214	-0.01686	0.6802

Born part, Fig. 4 (a), (b), and from the spectral function  $A_R(\cdot)$ . The contribution from the spectral function is almost constant and very small. The contribution from nucleon pole term depends very weakly on  $B$ .

Observable  $a$  is not well adjusted due to the huge contribution from  $A_R(\cdot)$ , being almost 75% of the final result. This huge contribution comes from negative part of the spectral function. We checked this point by doing  $A_R(\cdot) = 0$  for  $\cdot < 0$  by hand and get a result 5 times smaller for  $a$ . As discussed previously, the negative enhancement is an effect due to the form factors. This is a limitation of the model, since as we fix the cutoffs to reproduce the isoscalar low-energy observables, we can not reproduce the isovector ones.

#### D. Partial waves and Phase-shifts

The total amplitude for  $N$  scattering may be decomposed into the isospin  $\frac{3}{2}$  and  $\frac{1}{2}$  channels. The isospin  $\frac{3}{2}$  and  $\frac{1}{2}$  amplitudes are related to the symmetric and antisymmetric amplitudes by

$$\begin{aligned} O^{(3=2)} &= O^{(+)} - O^{(-)}; \\ O^{(1=2)} &= O^{(+)} + 2O^{(-)}; \end{aligned} \quad (60)$$

where  $O$  can be  $A$  or  $B$ . Therefore, the  $T$  matrix can be decomposed into good isospin and total angular momentum channels to reveal the existence of any resonances. The angular momentum decomposition of  $T$  leads to [26]:

$$\begin{aligned} f_l^I(W) &= \frac{1}{16W} \int_{-1}^1 dx (E+M) A^I(W; x) + (W-M) B^I(W; x) P_l(x) \\ &\quad + (E-M) A^I(W; x) + (W+M) B^I(W; x) P_{l+1}(x); \end{aligned} \quad (61)$$

where  $f$  is the partial wave amplitude,  $l$  is the orbital angular momentum, and  $I$  is the isospin.

From Eq. (60) one sees that the  $I = \frac{1}{2}$  channel is the result of a sum over symmetric and antisymmetric channels, which led to an imaginary part on the partial amplitude due to the pole for  $\cdot = \frac{1}{2}$  on  $A$  and  $B$  amplitudes, Eqs. (56,57). This fact does not happen in the  $I = \frac{3}{2}$  channel due to the amplitude subtraction in Eq. (60), which cancels the  $s^{-2}$  denominator. Thus, this approach cannot represent any of the  $I = \frac{3}{2}$  resonances, unless some kind of unitarization is made.

We can now define the scattering length ( $a$ ) in terms of the partial wave amplitude ( $f$ ). For each  $l$  value we can expand  $f$  in terms of  $q$  near the threshold ( $q = 0$ ) and write

$$a_l^I = \lim_{q \rightarrow 0} \frac{f_l^I}{q^{2l}}; \quad (62)$$

One observes that for the  $S$  wave ( $l = 0$ ), the scattering length is the partial wave amplitude at the threshold,  $a_{0+}^I = f_{0+}^I(q = 0)$ .

From the unitarity condition on the  $S$  matrix, we can relate the partial wave amplitude ( $f$ ) and the phase shifts ( $\delta$ ) as

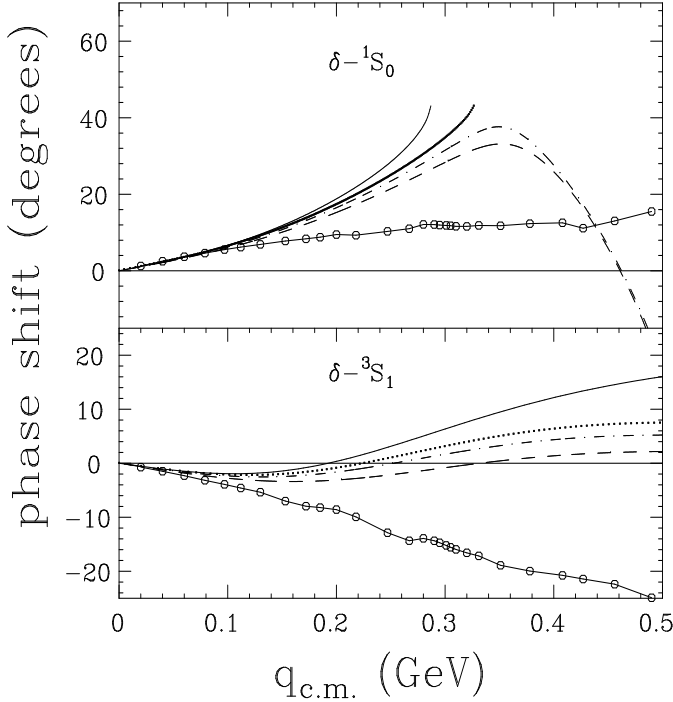


FIG. 5. Phase shifts for  $l=0$  waves. The curves represent the choices for the  $\pi$ -meson mass: 550 MeV (dashed), 770 MeV (dot-dashed), 980 MeV (dotted), and  $m_\pi = 1$  (solid curve). Data are from [1].

$$f_l^+ = \frac{e^{i\delta_l^+}}{q} \sin \delta_l^+ : \quad (63)$$

The optical theorem identifies the total cross section with the imaginary part of the scattering amplitude. We unitarize the amplitude following the method of Ollson and Ouspowski [32]. In their method, the real amplitude that arises from the model,  $m_l$ , is associated with the real part of the partial wave amplitude  $f_l^+$  as:

$$m_l^+ = \text{Re } f_l^+ = \frac{\sin 2\delta_l^+}{2q} \quad (64)$$

$$\delta_l^+ = \frac{1}{2} \arcsin 2qm_l^+ \quad (65)$$

Fig. 5 presents the results for the phase shifts for  $l=0$  waves. The agreement near threshold is very good, and the model fails for higher energies. The other phase shifts show the same trend: they are well described near threshold, but as energy increases the agreement with data becomes poor.

A much better agreement for the phase shifts can be achieved if we choose another set of values for the cut-offs [35], but the good agreement for the low-energy observables is destroyed.

Previous studies of  $N$  scattering by Nutt and Willets showed that in a model with  $\pi$  and  $\eta$  mesons the inclusion of the ghost poles lead to a much better agreement with experiment than if the poles were neglected. The fact that the Adler consistency condition could be satisfied in this approach is very intriguing since while one would expect that low energy observables should be insensitive to the ultraviolet (after renormalization), ghosts are a consequence of the ultraviolet behavior of the interaction kernel in the Hartree-Fock approximation. However, when we combine the  $A^+$  and the  $a^+$  observables, the ghost poles play no longer a special role, since the  $a^+$  experimental result can not be reproduced by this first approach. One natural solution to this problem is to modify the model in order to include chiral symmetry. In this paper we apply this idea in the light of the linear model augmented with the  $\eta$  meson. The solution of the nucleon Schwinger-Dyson equation obtained in the Hartree-Fock approximation in this approach also contains a pair of ghost poles. Moreover, the sum of ghosts plus  $\pi$  contribution exceeds by a large amount the experimental values of the  $a^+$  scattering length, leading to the conclusion that the ghosts are due to the approximations adopted. By definition, the scattering amplitude for the  $N$  interaction in the linear model has the correct chiral limit at the three-level calculations. As our calculations include loops, one needs to add additional terms in the lagrangian, to make sure that the resulting amplitude has the correct chiral limit. At the same time, it is possible to choose the constants of these additional terms in order to kill the complex poles. We intend to present this study in a near future.

In order to eliminate the ghosts, we used phenomenological form factors at the vertex interactions. In softening the ultraviolet by means of form factors it is possible to obtain qualitative agreement with experimental data of observables at low energies. The first observation from our study is that the spectral function  $A(\omega)$  for negative  $\omega$  is strongly enhanced by the form factors and this affects some of the observables. In particular, the negative enhancement increases the isospin antisymmetric scattering length  $a_-$ . Another lesson from this phenomenological model is that the phase shifts are well described only at threshold if we keep the cutoff values that reproduces the low-energy observables. One first conclusion is that it is almost impossible to reproduce together the observables at low and intermediate energies in  $N$  interaction with this simple phenomenological model, even including the fluctuations in the nucleon propagator.

In view of the compelling evidences that chiral symmetry is a fundamental symmetry of the strong interactions, the problem of the appearance of ghost poles at low energies in commonly used truncation schemes in field theoretic models has to be very carefully examined before definite conclusions can be drawn on the valid-

ity of a particular model used for the description of the data. One has believed that Chiral Perturbation Theory (CHPT) is the unique solution, in the near future, to all these requirements, since it clearly states how to add loops and keep the chiral limits of the low-energy observables. However, to describe data at intermediate energies, one needs to evaluate diagrams with 2 or maybe more loops, which are very involved due to the regularization process done in every order. Moreover, the number of unknown constants increase with the number of loops, compromising the predictive power of the theory.

We believe that much still remains to be studied with respect to the interplay of chiral symmetry and the ultraviolet behavior of the model interactions. One particular issue is the role of vertex corrections in the Schwinger-Dyson equation and the requirement that these should satisfy the chiral Ward-Takahashi identities. Such constraints are expected to be relevant at the low-energy region of the kernel interactions and as such can be of importance for a better fit to experimental data at low energies.

#### ACKNOWLEDGMENTS

We thank Prof. M. Robilotta and Prof. T. Cohen for helpful conversations about  $N$  scattering and chiral symmetry. This work was partially supported by U.S. Department of Energy. The work of C.A. da Rocha, was supported by CNPq Grant No. 200154/95-8 and (in the early stages of this work) by FAPESP Grant No. 92/5095-1, both Brazilian agencies.

---

[1] G. Hohler, Pion-nucleon scattering, in Landolt-Bornstein, Vol. I/9B-2, (H. Schopper, ed., Springer Verlag, Heidelberg, 1983).

[2] B.C. Pearce and B.K. Jennings, Nucl. Phys. A 528, 655 (1991).

[3] F. Gross and Y. Surya, Phys. Rev. C 47, 703 (1993).

[4] P.F.A. Goudsmit, H.J. Leisi, and E. Matsinos, Phys. Lett. B 299, 6 (1993).

[5] M. Lacombe, B. Loiseau, J.M. Richard, R. Vinh Mau, J. Côté, P. Pires, and R. de Tourreil, Phys. Rev. C 21, 861 (1980); V.G.J. Stoks, R.A.M. Kemper, M.C.M. Rentmeester, and J.J. de Swart, Phys. Rev. C 48, 792 (1993).

[6] R. Machleidt, K. Holinde, and Ch. Elster, Phys. Rep. 149, 1 (1987).

[7] J. Gasser, M.E. Sainio, and A. Svarc, Nucl. Phys. B 307, 779 (1988).

[8] E. Jenkins and A.V. Manohar, Phys. Lett. B 255, 558 (1991).

[9] G. Ecker, Phys. Lett. B 336, 508 (1994).

[10] J. Gasser, H. Leutwyler and M.E. Sainio, Phys. Lett. B 253, 252 (1991).

[11] S. Weinberg, Nucl. Phys. B 363, 3 (1991).

[12] P.A.M. Dirac, Proc. R. Soc. London, Ser. A 180, 1 (1942); W. Pauli and F. Villars, Rev. Mod. Phys. 15, 175 (1943); 21, 21 (1949); T.D. Lee, Phys. Rev. 95, 1329 (1954); E.C. Sudarshan, Proceedings of the 14th Solvay Conference, Brussels, Belgium, 1967 (Interscience, New York, 1968).

[13] W.D. Brown, R.D. Puthoff, and L. Wiets, Phys. Rev. C 2, 331 (1970).

[14] L. Wiets, in Mesons in Nuclei, (M. Rho and D. Wilkinson eds., North-Holland, Amsterdam, 1979).

[15] R.J. Perry, Phys. Lett. B 199, 489 (1987); T.D. Cohen, M.K. Banerjee, and C.-Y. Ren, Phys. Rev. C 36, 1653 (1987); K. W. Ehrberger, R. Williams, and B.D. Serot, ibid. 42, 2680 (1990).

[16] G. Krein, M. Nielsen, R.D. Puthoff, and L. Wiets, Phys. Rev. C, 47 2485 (1993).

[17] J. Milana, Phys. Rev. C 44, 527 (1991).

[18] M.P. Allendes and B.D. Serot, Phys. Rev. C 45, 2975 (1992).

[19] M.E. Bacco, A. Eiras, G. Krein, and L. Wiets, Phys. Rev. C 49, 1299 (1994).

[20] W.T. Nutt and L. Wiets, Phys. Rev. D 11, 110 (1975).

[21] S. Adler, Phys. Rev. 137, B1022 (1965).

[22] S. Weinberg, Phys. Rev. Lett. 17, 616 (1966).

[23] M. Gell-Mann and M. Levy, Nuovo Cimento 16, 705 (1960).

[24] B.J. Lee, Chiral Dynamics, (Gordon and Breach, New York 1972).

[25] S.S. Schweber, An Introduction to Relativistic Quantum Field Theory, (Harper & Row, Publ., New York, 1962).

[26] P. Roman, Introduction to Quantum Field Theory, (John Wiley & Sons, Inc., New York, 1969).

[27] N.N. Bogolubov, A.A. Logunov, and I.T. Todorov, Axiomatic Quantum Field Theory, (Benjamin, Reading MA, 1975, pp. 269-270, 330, Appendix F).

[28] B.D. Serot and J.D. Walecka, Adv. in Nucl. Phys., Vol. 16, (J.W. Negele and E. Vogt eds., Plenum Press, New York, 1986).

[29] C.A. da Rocha and M.R. Robilotta, Phys. Rev. C, 49, 1818 (1994); 52, 531 (1995).

[30] N.A. Tornqvist and M. Roos, preprint hep-ph 9511210.

[31] F. Gross, J.W. Van Orden, and K. Holinde, Phys. Rev. 45, 2094 (1992).

[32] M.G. Olsson and E.T. Ojowski, Nucl. Phys. B 101, 136 (1975).

[33] S.A. Coon, M.D. Scadron, P.C. McNamara, B.R. Barrett, D.W.E. Blatt, and B.H.J. McKellar, Nucl. Phys. A 317, 242 (1979).

[34] S.A. Coon, and W. Glockle, Phys. Rev. C 23 1790 (1981).

[35] G. Krein, Private communication (1996).